

Influence of Pretreatment on Adhesion Quality of Supercritical-fluid-deposited Cu Film on Si

Naoto Usami,^{1†} Etsuko Ota,^{2*†} Takeshi Momose,³ Akio Higo,² and Yoshio Mita^{1,2}

¹Department of Electrical Engineering and Information Systems, Graduate School of Engineering,
The University of Tokyo, 7-3-1 Hongo, Bunkyo-ku, Tokyo 113-8656, Japan

²VLSI Design and Education Center, The University of Tokyo,
2-11-16 Yayoi, Bunkyo-ku, Tokyo 113-0032, Japan

³Department of Materials Engineering, Graduate School of Engineering, The University of Tokyo
7-3-1 Hongo, Bunkyo-ku, Tokyo 113-8656, Japan

(Received January 28, 2019; accepted April 18, 2019)

Keywords: supercritical fluid deposition (SCFD), Cu thin film, surface pretreatment, adhesion, tape test, high-aspect-ratio nanostructures (HARNS)

In this paper, we report on the impact of sample preparation methods on the adhesion reproducibility of thin films, considering future applications of supercritical fluid deposition (SCFD) to MEMS/NEMS with high-aspect-ratio micro- and nanostructures (HARMS/HARNS). Our experiments revealed the importance of careful cleaning before SCFD. The Cu on the samples treated with appropriate cleaning and drying sequences could stick to the sample enduring the adhesive pull-out test. By using a silicon substrate, we confirmed that sample surface contaminations were reduced by cleaning, as observed by a decrease in the carbon peak in field emission Auger electron spectroscopy (FE-AES). At the same time, a subtle roughness increase (of 0.2 nm RMS) after a series of cleaning steps was confirmed by scanning probe microscopy (SPM/AFM) measurement. On the basis of the acquired knowledge, Cu SCFD on Si surfaces was studied. A relatively low temperature (130–150 °C) deposition condition was obtained, with which the produced Cu films exhibited high adhesion on all samples. The deposition of 100-nm-thick Cu was successfully demonstrated on the sidewalls of a Si trench with 450 nm width and 22.5 μm depth (aspect ratio of 50).

1. Introduction

In the history of electron device development, process and device technologies have been reciprocally stimulated. In other words, a new device inspired a new technology that in turn became the basis of yet another new device. For example, to improve a MEMS physical sensor such as an accelerometer, deep reactive ion etching (DRIE) apparatuses as well as the Bosch Process were developed,⁽¹⁾ thus the DRIE process has become a key enabling technology in creating so-called high-aspect ratio micro- (and later nano-) structures (HARMS/HARNS).⁽²⁾ Many new devices such as MEMS and through-silicon vias (TSVs)⁽³⁾ have been

*Corresponding author: e-mail: ohta@if.t.u-tokyo.ac.jp

†Equally contributed.

<https://doi.org/10.18494/SAM.2019.2316>

invented. Since the beginning of the 21st century, “new open-platform policies”⁽⁴⁾ in micro- and nanofabrication facilities have been created in several countries, such as the National Nanotechnology Infrastructure Network (NNIN) in the USA, RTB-RENATECH in France, and Nanotechnology Platform in Japan. The engineers of the platform, including us, are standing on the technological side and are looking for such reciprocal development of new technologies and devices. To achieve such a goal, we are endeavoring to make new cutting-edge processes accessible as highly reliable common platform technologies.

In this paper, we report a supercritical fluid deposition (SCFD) of copper (Cu). The SCFD was proposed as a deposition method having excellent in-step coverage on a microstructure.⁽⁵⁾ Carbon dioxide is used as a reaction medium in this study. Carbon dioxide is in the gas phase at room temperature and is solid at low temperature; in the supercritical phase appearing above its critical temperature and pressure, high density, high solubility,⁽⁶⁾ and low viscosity can be simultaneously obtained. Most importantly, since there is no surface tension in supercritical fluid, materials can be transported deep into HARNS. In such a way, if the extremely small pores or deep grooves (trenches) formed by etching are backfilled with various metallic materials such as copper, nickel, permalloy, and gold, such materials can then be further used as structural components (Fig. 1) of mechanical and/or electrical devices. The deposited layer may also be used as a conductive seed layer for electroplating to fill wider trenches, analogous to oxide trench refilling, known as the damascene process.⁽⁷⁾ In general, the seed layer of TSV is deposited by sputtering, but because sputtering is a physical deposition, the step coverage on the trench surface of HARNS⁽³⁾ is poor. Atomic layer deposition is an alternative method for better step coverage owing to the cyclic precursor supply sequence, although the cyclic sequence results in a low growth rate (for example, around 0.2 nm/min for Cu on thermal SiO₂⁽⁸⁾).

In this study, we experimentally found process procedures that provide reliable thin films, referred here to as sufficiently adherent films useable for the following processes, for example, electroplating and polishing. We report SCFD characteristics evaluated by six testing methods: peeling-off test of adhesive tape for confirmation of adhesion and field emission Auger electron spectroscopy (FE-AES) for element analyses of both the surface and the depth profile.⁽⁹⁾ They are complementary to standard evaluation methods: An electrical circuit tester for conductivity, SPM for surface flatness measurement, and cross-sectional scanning electron microscopy

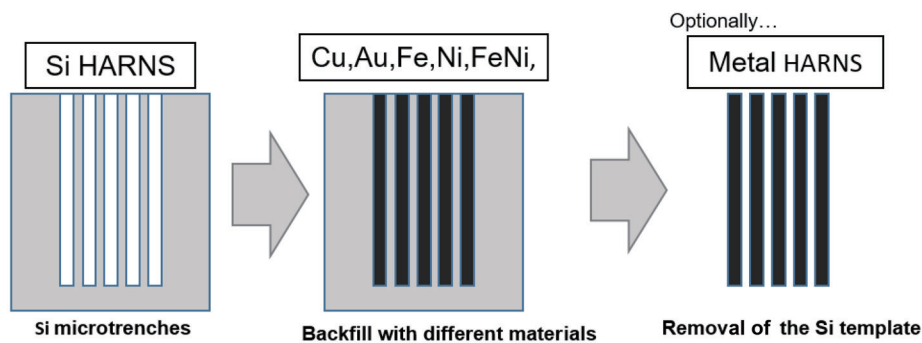


Fig. 1. (Color online) Embedding technology into Si microtrenches expands the applicability of metal materials as microstructures.

(SEM) for confirmation of film thickness⁽¹⁰⁾ were used. The real difficulty has been that, during our development, there often were samples that did not pass the adhesion tape test even though we took care of keeping them as much as possible, and the film characteristics other than adhesion were as good as the values reported in the literature.⁽¹¹⁾ The experiments were carried out in the new equipment installed in another cleanroom to serve as an open platform machine. During the installation, we realized that the adhesion property may sometimes differ from one machine to another. We have therefore taken care to improve the machine quality to be as good as in our past experiences. The resulting machine configuration, as well as SCFD procedure, is summarized in Sect. 2. Regarding adhesion, we empirically know from past experience that SCFD on nonmetallic surfaces often suffers from low adhesion, whereas on metallic surfaces, adhesion is good. By further looking into the causes, we identified that one of the root causes was in the cleaning procedure of the sample before SCFD. We could not find papers that specifically underlined the importance of cleaning, probably because the cleaning procedure is rather trivial (but important in practice). However, surface characteristics depend on the cleaning procedure. The surface condition of a Si substrate, which is not only the extent of contamination but also conductive-or-insulative (Si or SiO₂), is especially determined by cleaning steps.

Underneath adjacent materials, reaction temperature and surface contamination strongly influence growth and film quality in SCFD as in previous works.^(12,13) Crystalline growth in SCFD often occurs on conductive surfaces.^(12,14) According to precursor and/or deposition condition, that on an insulator such as SiO₂ including native oxide on Si substrates, can also be observed.⁽¹²⁾ Cabañas *et al.* presented that a high reaction temperature was required for direct SCFD on an insulator. They also demonstrated Au SCFD on SiO₂,⁽¹⁵⁾ and CuMn_xO_y SCFD on SiO₂ was reported by Uejima *et al.*⁽¹⁶⁾ Although direct Cu SCFD on SiO₂ was also demonstrated,⁽¹⁷⁾ a Cu film on SiO₂ has very poor adhesivity.⁽¹⁸⁾ Inserting an adhesion layer can contribute to the improvement of adhesion on a SiO₂ surface.⁽¹⁸⁾ An supercritical fluid (SCF)-deposited Cu film on a conductive surface, for example, OsO_x, TiN, and Ru, has better adhesivity than that on SiO₂,^(19,20) and high adhesivity according to such adjacent layers permits an additional process such as CMP.⁽²¹⁾ Surface contamination in SCFD is reported to be the cause of poor adhesion.⁽²²⁾ SCFD film quality also depends on other deposition conditions such as precursor material and its amount, as well as supercritical CO₂ (scCO₂) and H₂ concentrations;^(22,23) they are set to be constant in this paper. Comparisons between SCFD and other deposition techniques were well investigated by Teraoka *et al.*⁽¹⁸⁾ and Giroire *et al.*,⁽²⁴⁾ which are excluded in this paper.

As mentioned above, adjacent materials and contamination strongly influence the result of SCFD. Therefore, SCFD on a Si substrate is highly affected by cleaning steps, which changes top-layer materials and contamination status. In this paper, we focus on the SCFD of Cu on Si substrates to experimentally assess the importance of cleaning steps. In Sect. 4, we evaluated surface conditions of Si substrates through step-by-step RCA cleaning procedures.⁽²⁵⁾ In Sect. 5, Cu SCFD on Si substrates was performed with various reaction temperatures to investigate the morphology and adhesivity of the SCF-deposited Cu film. Finally, by using the obtained optimal cleaning condition, a SCFD over a 450-nm-wide, 22.5-μm-deep Si trench is demonstrated to show the step coverage of SCFD.

2. Experimental Procedure

2.1 SCFD equipment

Figures 2 and 3 show a schematic diagram of the experimental equipment designed for this research and photographs of the reaction chamber, respectively. We made a batch deposition system. In addition to the substrate, the following materials were put into the airtight chamber: carbon dioxide as the reaction medium, hydrogen as the reducing agent, and a metal precursor as the film-forming material compound and particle filter as well as the CO₂ desiccant tube (filled with zeolite) are put in the line. The chamber outlet is connected to both the dry pump for predeposition chamber treatment and the abatement system for postreaction chemical treatment. A pressure gauge (PHC-B-20MP adjusted to a maximum of 30 MPa) is connected to the chamber. The substrate temperature is controlled using a PID controller (TJA-450K, 0–399 °C) with a heater for the chamber and a temperature monitor inserted into the chamber, along with a cooling fan switched on/off manually.

The following analyses apparatuses were used. SAM-680 FE-AES from ULVAC-PHI Inc. was used for surface depth element analyses. L-TraceII from Hitachi High-Technologies Corp. (HHT) was used for SPM in the tapping mode. The curvature radius of the SPM tip was 7 nm. The measurement mode of L-TraceII was set to a special mode called the sampling intelligent

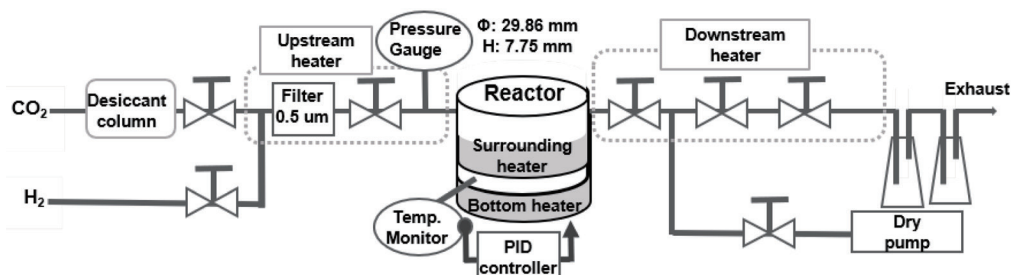


Fig. 2. Block diagram of SCFD system (made in-house).

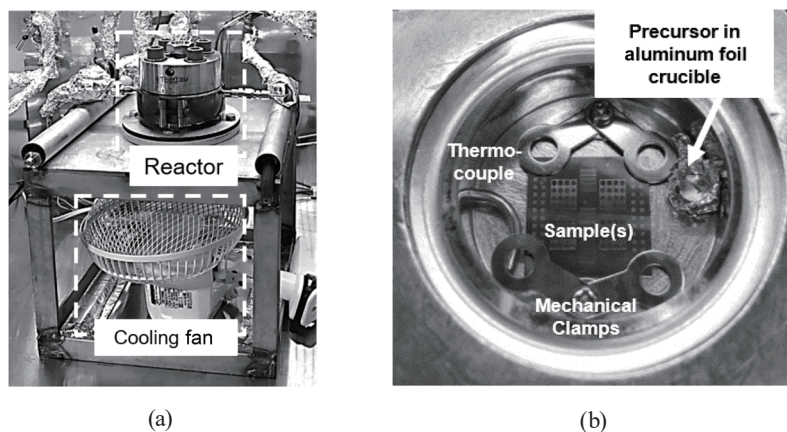


Fig. 3. Photograph of SCFD equipment. (a) Overview and (b) deposition chamber.

scan (SIS) mode. Under the SIS mode, tapping is performed only at the region of measurement and the cantilever tip is evacuated to about 10 nm above the surface at the other places, whereas general tapping is done throughout regardless of the position (region of measurement and elsewhere). We know from a previous experiment that when using the SIS mode, a sharp edge can be taken while reducing the damage on the sample and the cantilever tip. The S-4700 SEM from HHT is used for surface and cross-sectional electron microscopy observations.

2.2 SCFD process

Figure 4(a) shows the experimental procedures. First, a silicon chip with the maximum size of $2 \times 2 \text{ cm}^2$ is prepared from a standard 4" wafer (525 μm thick). Cleaning details will be explained in each following section. A chip and a copper precursor powder, bis(2,2,6,6-tetramethyl-3.5-heptanedionate),⁽⁶⁾ were placed in the precursor crucible in the chamber and firmly clamped with a torque wrench. The weight of Cu in the precursor, w_{Cu} , was varied, where 10 mg of precursor was equivalent to 0.002 mol/L. The reactor was then pumped down with a dry pump for five minutes. The initial pressure for H_2 (p_{IH_2}) was from 0.5 to 1.0 MPa, and that of CO_2 (p_{ICO_2}) was from 7.0 to 11 MPa at 50 °C. Figure 4(b) shows the typical temperatures and corresponding pressures during the reaction. After a 10 min holding time for stabilization, the temperature was increased (called boost step) with a heater to the target temperature (T_T), which was maintained for a while (t_T) (typically 10 to 30 min). The reaction mainly occurred during t_T . The ultimate pressure p_T during the reaction was 20 to 25 MPa. Then the pressure was gradually released while cooling the chamber, and coated samples were subsequently analyzed.

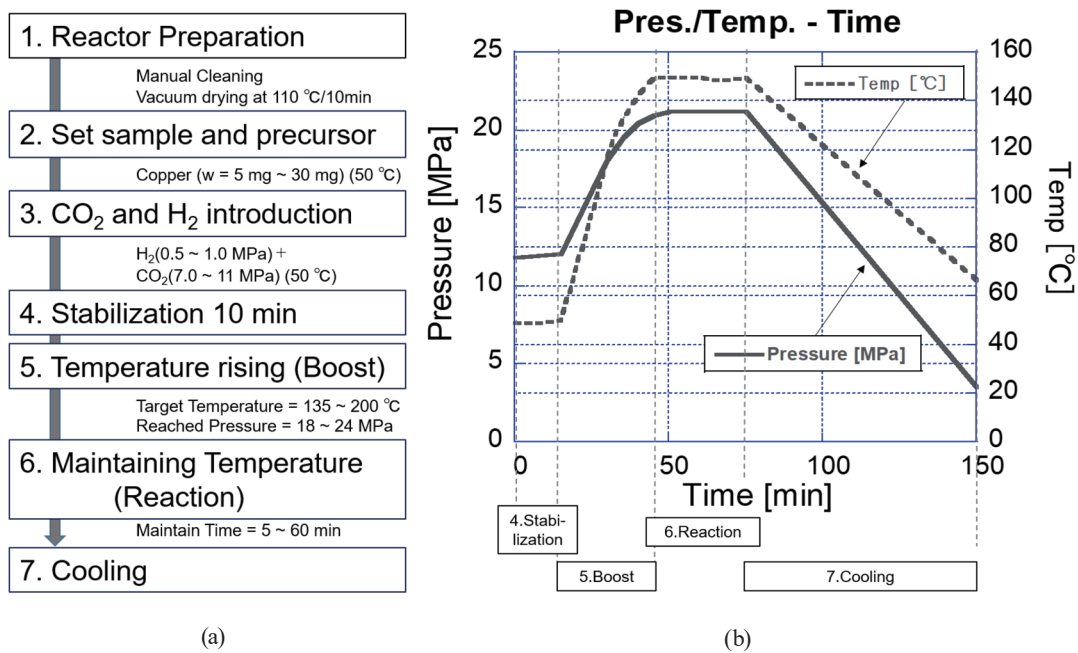


Fig. 4. (Color online) Deposition procedure. (a) Flow chart. (b) Typical temperature and corresponding pressure.

3. Effect of Substrate Cleaning on Reproducibility of SCFD-Cu Film Adhesion

3.1 Impact of substrate cleaning

Figure 5(a) shows the “tape test” method that we used to evaluate adhesion. Adhesive tape is put on the substrate after SCFD and then peeled off. The peeling angle is kept at 90°. Figure 5(b) shows three test chips with different cleaning conditions. Chips A-1, A-2, and A-3 were made from the same silicon wafer. Chips A-1 and A-2 were cleaned by our standard procedure (BHF, APM, and baking. Cleaning details are explained in Sect. 3.2). The SCFD was performed on sample A-1 as soon as the cleaning was finished. Sample A-2 was left in the clean room for one night before the SCFD. Another SCFD was made on sample A-3, which was not cleaned (just left as-is delivered). The conditions are listed in Table 1. As clearly seen in Fig. 5(b), the deposited Cu on sample A-2 had such a weak adhesion that the Cu was peeled off by both an adhesive tape and soft wiping. On the sample with no cleaning (A-3), Cu did not deposit. Only the SCFD Cu on the properly cleaned sample (A-1) exhibited good adhesion;

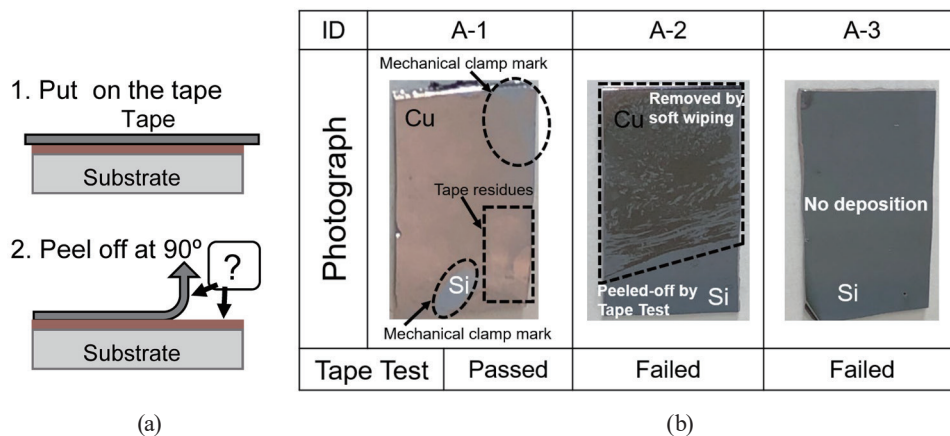


Fig. 5. (Color) (a) Tape test method and (b) example results.

Table 1
Process conditions for samples shown in Fig. 5.

Sample ID	A-1	A-2	A-3
Surface Material	Si	Si	Si
Description	APM, BHF, just before SCFD	APM, BHF left in cleanroom for one night	With no cleaning procedure
Conditions (w_{Cu} , p_{IClO_2} , p_{IH_2} , T_{T} , p_{T} , t_{T})	5 mg, 11.24 MPa, 1.01 MPa, 20.23 MPa, 150 °C, 10 min	5 mg, 10.95 MPa, 1.00 MPa, 20.42 MPa, 150 °C, 10 min	5 mg, 10.83 MPa, 1.00 MPa, 20.00 MPa, 150 °C, 10 min
Tape test	Passed	Failed (weak adhesion)	Failed (no deposition)

APM: ammonium hydrogen peroxide mixture

BHF: buffered hydrofluoric acid

after the tape test, not only the Cu film remained on the entire surface but also tape residues remained on some areas. The importance of surface treatment prior to SCFD was thereby demonstrated.

3.2 Comparison of properties of SCFD-Cu film deposited on substrates cleaned by various cleaning methods

To investigate the impact of cleaning on SCFD, we performed two comparative studies using two identical Si substrates (samples B-1 and B-2). They were made from a 1.0–10.0 Ωcm, 525-μm-thick 4” wafer. The chip size was 10 × 10 mm². Two different cleaning methods were applied, then the chips were placed simultaneously in the chamber and SCFD was performed. The evaluation of characteristics includes the conductivity test, adhesion tape test, root-mean-square (RMS) surface roughness, and peak-to-valley (P–V) value by SPM (area was 1 × 1 μm²). The results are summarized in Table 2.

Table 2 shows Si substrate measurements. Chip B-1 was immersed in 15% buffered HF (BHF 110) for 30 s, and then immersed three times in deionized (DI) water for 1 min each. This standard “light” cleaning procedure is expected to remove native oxide. As a comparison, chip C-2 was cleaned more heavily: ammonia hydrogen peroxide cleaning (APM cleaning) with a mixed solution of ammonium water 29% (NH₃):H₂O₂:DI water = 1:1:5 at 170 °C for 10 min, followed by three repetitions of DI water cleaning for 1 min each. The sample was then immersed in 15% BHF for 10 min, followed by two repetitions of DI water cleaning for 2 min each. After cleaning, the samples were dried by baking at 180 °C for 5 min on a hot plate. In these cleaning methods, a continuous film was grown.

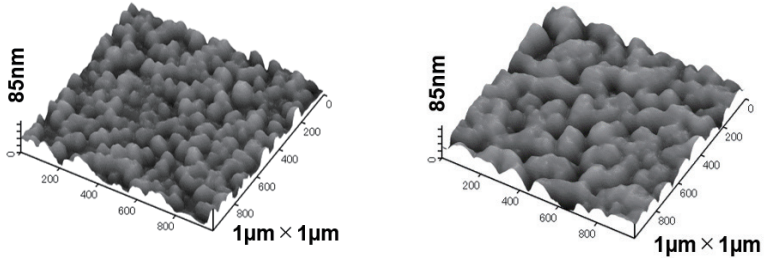
By summarizing the results for samples B-1 and B-2, we learned the following.

- Cleaning is important: Insufficient cleaning may lead to insufficient adhesion of the SCFD film.

Table 2
Characteristics of SCFD of Cu on Si surface cleaned by different cleaning methods.

Sample ID	B-1	B-2
Description	BHF 30 s cleaning	BHF 10 min + APM 10 min
Conditions (w_{Cu} , T_T , t_T)	10 mg, 140 °C, 30 min	10 mg, 140 °C, 30 min
Tape test	Failed	Passed

SPM image



RMS	11.59 nm	11.08 nm
P–V	62.66 nm	59.43 nm

- On a bare silicon surface, only BHF cleaning did not contribute to adhesion, which means that there are not only native oxide but also some unknown contaminants that prevent adhesion. APM cleaning can efficiently remove such contaminations.
- For a metal surface, thorough solvent cleaning could increase adhesion.

4. Materials and Morphological Investigation of Substrates Subjected to Different Cleaning Methods.

The experiments in the previous section revealed the importance of careful cleaning in increasing the adhesion. Here, a question arises: “How complete should we be? What is the impact of cleaning?” To answer the questions, we examined samples subjected to different steps of RCA-style⁽²⁵⁾ cleaning.

4.1 Experimental condition

Twelve samples of $10 \times 8 \text{ mm}^2$ were prepared from the same silicon wafer (boron-doped, $1\text{--}10 \text{ }\Omega\text{cm}$, $525\text{-}\mu\text{m}$ -thick 4” wafer). They were cleaned by the cleaning sequence summarized in Table 3. There were six different conditions, from no cleaning (C-1 and C-2) to complete RCA cleaning (H-1 and H-2). Samples with the suffix -1 were measured by FE-AES under both surfaces (area of $700 \times 600 \text{ }\mu\text{m}^2$) and in-depth material profile (area of $50 \times 50 \text{ }\mu\text{m}^2$). Those with the suffix-2 were examined by SPM (area of $1 \times 1 \text{ }\mu\text{m}^2$).

For sequence 1, the sample immersed in the ethanol solution was subjected to ultrasonic cleaning for 10 min at room temperature (RT). For sequence 2, the substrate was placed in a mixed liquid of $\text{H}_2\text{SO}_4\text{:H}_2\text{O}_2 = 3\text{:}1$ at $150 \text{ }^\circ\text{C}$ for 10 min with a lid for sulfuric acid cleaning (“piranha” cleaning). Then the substrate was dip-rinsed twice in DI water for 1 min each and further rinsed with flowing DI water for 5 min. For sequences 3 and 5, 15% BHF110 at room

Table 3
Cleaning sequences. None: sequence not performed.

	Sequence/Description				
	Sequence 1	Sequence 2	Sequence 3	Sequence 4	Sequence 5
	Ethanol solution using ultrasonic cleaning	Sulfuric acid hydrogen peroxide mixture (“piranha”)	Buffered hydrofluoric acid (BHF)	Ammonium hydrogen peroxide mixture (APM)	BHF
	$\text{C}_2\text{H}_5\text{OH}$. Room temperature (RT)/10 min.	$\text{H}_2\text{SO}_4\text{:H}_2\text{O}_2 = 3\text{:}1$. $150 \text{ }^\circ\text{C}/10 \text{ min.}$	BHF110 15%. RT/10 min.	$\text{NH}_4\text{OH:H}_2\text{O}_2\text{:H}_2\text{O} = 1\text{:}1\text{:}5$. $170 \text{ }^\circ\text{C}/10 \text{ min.}$	BHF110 15%. RT/10 min.
ID					
C-1/C-2	None	None	None	None	None
D-1/D-2	○	None	None	None	None
E-1/E-2	○	○	None	None	None
F-1/F-2	○	○	○	None	None
G-1/G-2	○	○	○	○	None
H-1/H-2	○	○	○	○	○

○: Sequence performed as described

temperature was used for ten minutes. The samples were then dip-rinsed in DI water twice, for 2 min each, and then rinsed with flowing DI water for 5 min. In sequence 4, APM cleaning was performed with a mixed solution of 29% ammonium water (NH_4OH): H_2O_2 :DI water = 1:1:5 at 170 °C for 10 min. The samples were dip-rinsed three times in DI water for 2 min each. After each rinse, the chips were dried on a hotplate at 180 °C for 5 min. Note that the SCFD-Cu thin film on a watermark (a.k.a. mark with water residue) peels off easily, so special care was taken in baking to not produce any watermarks.

4.2 Material analyses by FE-AES

The effect of cleaning was verified by FE-AES. The surface depth profile was analyzed for each sample surface. AES is the spectroscopic analysis of Auger electrons induced by an electron beam. Spectral information of the materials at the surface can be obtained. By scanning the incident electron beam, 2-D mapping of a material is possible. Measurement conditions were 10 kV, 10 nA, 3 cycles, and area of $700 \times 600 \mu\text{m}^2$. The apparatus used in the experiment (PHI 680) has an argon milling system. By alternating etching and AES, it is possible to obtain in-depth material distribution information. The survey conditions were as follows: 3 kV, $1 \times 1 \text{ mm}^2$, area of $50 \times 50 \mu\text{m}^2$, sputter interval of 30 s, and milling time of 10 min. The sputtering (etching) rate is reported to be 3.58 nm/min for SiO_2 .

Raw spectral data obtained in the survey mode for samples C-1 to H-1 are summarized in Fig. 6. Peaks corresponding to Si, O, and C were identified. These spectra were then converted into atomic concentration of elements, as shown in Fig. 7. Decrease in oxygen concentration is found in samples F-1 and H-1. This corresponds to the removal of oxide from the samples cleaned with BHF. Also, the increase in oxide concentration in sample H-1 confirms the occurrence of oxidation during cleaning (by hydrogen peroxide). In the end, after all the cleaning sequences, only 3.37% oxygen was observed on the Si substrate.

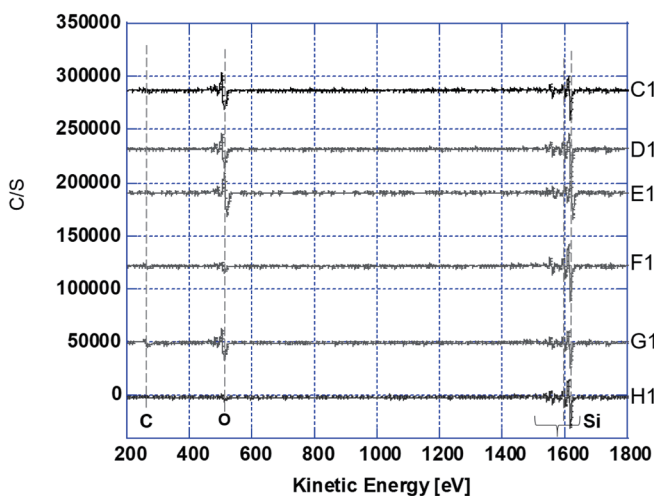


Fig. 6. (Color online) Energy spectral data obtained by FE-AES (in survey mode).

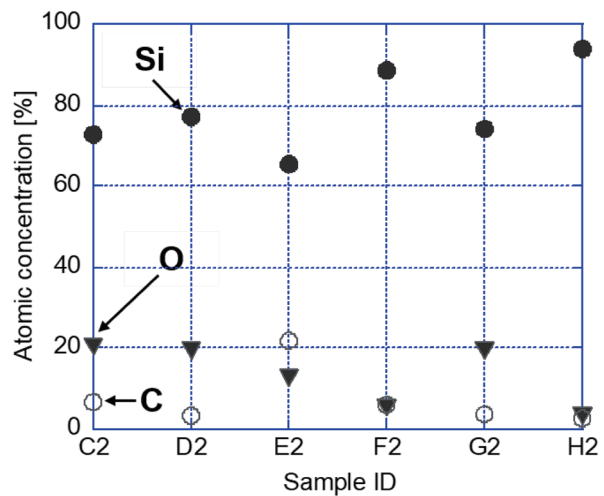


Fig. 7. (Color online) Atomic concentrations of Si, O, and C after each cleaning step.

Figure 8 shows the depth profiles measured by FE-AES coupled with argon sputtering. The depth profiles confirm that contaminating materials (measured as carbon) exist at the surface. The atomic concentrations of oxygen and carbon decreased as cleaning progressed. As summarized in Table 4, the oxygen concentration decreased from 28.43% (C-1) to 4.74% (H-1) and the carbon concentration decreased from 7.24% (I-1) to 6.60% (H-1). The large carbon concentration in the sample (G-1) indicates that there were particles on the surface, but such contamination can be removed by BHF cleaning as shown in Fig. 8(f). The removal of contaminating materials such as carbon is thereby confirmed. Therefore, organic cleaning + APM + BHF is sufficient to remove metallic contamination, carbon contamination, and native oxide.

4.3 Surface roughness assessment by SPM

The surface roughness was measured using samples C-2 to H-2. The samples were cleaned by the same procedure as shown in Table 3. After each cleaning sequence, the substrates were measured by SPM.

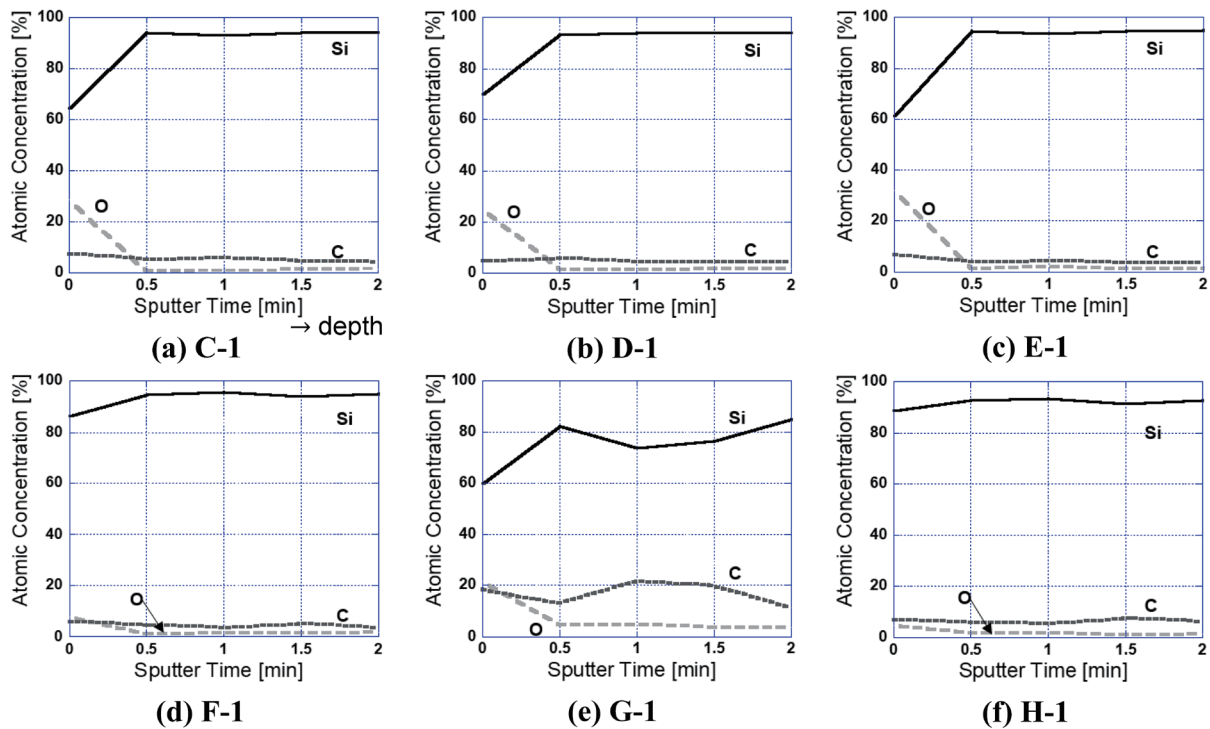


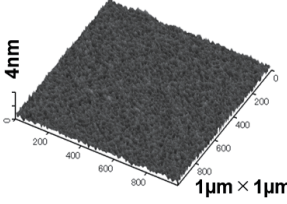
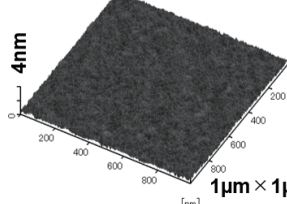
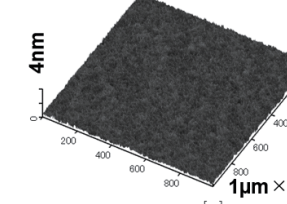
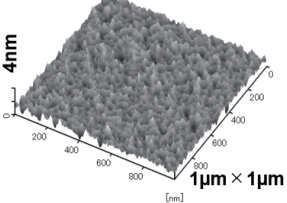
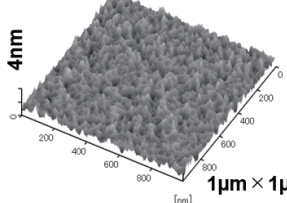
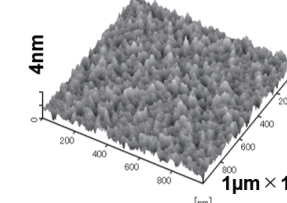
Fig. 8. (Color online) Depth profiles of Si, O, and C on samples at different cleaning steps.

Table 4

Concentration evolution of contaminating material with cleaning.

Material	Concentration in sample C-1 (%)	Concentration in sample H-1 (%)
O	28.43	4.74
C	7.24	6.60

Table 5
SPM images and surface roughness values.

ID	C-2	D-2	E-2
Description	No cleaning	After ethanol cleaning	After “piranha” cleaning
SPM image			
RMS	0.18 nm	0.13 nm	0.13 nm
P-V	1.94 nm	1.35 nm	1.10 nm
ID	F-2	G-2	H-2
Description	After BHF	After APM cleaning	After BHF
SPM image			
RMS	0.32 nm	0.30 nm	0.38 nm
P-V	2.63 nm	2.44 nm	3.90 nm

Measurement results are summarized in Table 5. The initial surface flatness value was measured with sample C-2 and were 0.18 nm in RMS roughness and 1.94 nm from the Peak to Valley (P-V). It was observed that (1) roughness decreases after “piranha” and APM cleaning steps (E-2 and G-2) and (2) roughness increases after BHF etching. From the oxygen concentration shown in Fig. 6 and the surface roughness, we can understand that “piranha” and APM cleaning causes oxidation of the silicon surface, and the SiO₂ contributes to reducing the surface roughness. This assumption is supported by the increase in the surface roughness after BHF cleaning (F-2 and H-2). At the end of the cleaning sequence (H-2), RMS and P - V values were 0.38 and 3.90 nm, respectively. In conclusion, cleaning using acid or base and hydrogen peroxide can remove contaminations such as carbon, but in return, the roughness of the substrate surface increases by around 0.2 nm.

5. Copper SCFD on Substrates with Optimized Cleaning

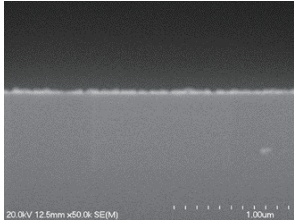
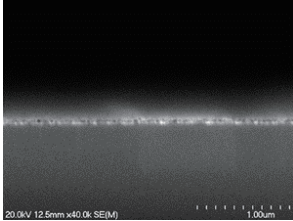
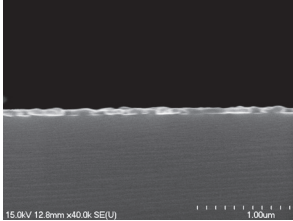
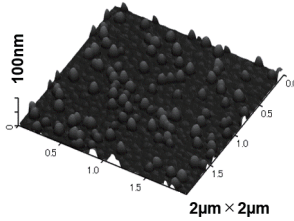
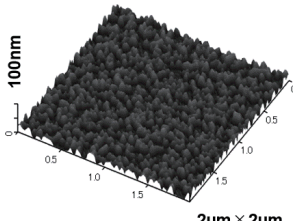
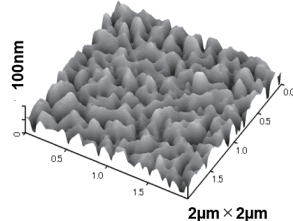
In this section, the dependence of SCFD-Cu growth on temperature is reported. We prepared three Si test chips: I-1, J-1, and K-1. By using the optimum conditions, a narrow trench refilling process (HARNS-damascene process) was demonstrated.

5.1 Copper SCFD Dependence on Temperature over Different Interface Materials

Careful cleaning was performed for all the samples taking into account the results described in Sect. 4; samples I-1, J-1, and K-1 were cleaned for 10 min in ethanol, 10 min in APM at 170 °C, and 10 min in BHF110, then baked for 5 min on a hotplate at 180 °C. The conditions correspond to those of sequences 1, 4, and 5 in Table 3. Note that the SCFD condition K-1 is identical to that of sample A-1.

The samples were then subjected to the tape test, conductivity test, cross-sectional SEM observation, and SPM measurement on an area of $2 \times 2 \mu\text{m}^2$. Measurement results for samples grown at 130, 140, and 150 °C are summarized in Table 6. The target initial CO₂ and H₂ pressure (p_{ICO_2} , p_{IH_2}) were 11 and 1 MPa, respectively; owing to the pumping procedure, the initial CO₂ pressure was varied by the maximum relative error of 1.78% (11.10 to 11.30 MPa). According to Fig. 3 of Ref. 6, the initial pressure influences solubility but the error can be estimated as 4.12% (4.76×10^{-3} to 4.76×10^{-3} mol/L). Therefore, we assume that the initial variance had a small influence on deposition.

Table 6
SCFD growth over different surfaces. Growth temperature at 130 °C

ID	I-1	J-1	K-1 (identical to A-1)
Description	Cu on Si at 130 °C	Cu on Si at 140 °C	Cu on Si at 150 °C
Conditions (w_{Cu} , p_{ICO_2} , p_{IH_2} , p_T , T_T , t_T)	5 mg, 11.11 MPa, 1.00 MPa, 16.32 MPa*, 130 °C, 10 min	5 mg, 11.30 MPa, 1.00 MPa, 20.94 MPa, 140 °C, 10 min	5 mg, 11.24 MPa, 1.01 MPa, 20.23 MPa, 150 °C, 10 min
Tape test	Passed	Passed	Passed
Conductivity	Conductive	Conductive	Conductive
Thickness	40 nm	45 nm	89 nm
Cross-sectional SEM			
			
RMS	8.18 nm	9.63 nm	18.60 nm
P-V	40.08 nm	44.22 nm	106.1 nm

*In this experiment, some leakage in the system was suspected. However, CO₂ under this pressure was in the supercritical phase; therefore, SCFD occurred.

At 130 °C, the deposited film was not continuous; as seen in the SPM image of sample I-1, nuclei of 2 to 20 nm height covered the surface entirely. In contrast, at 140 and 150 °C, the grown film was continuous for the tested samples J-1 and K-1. These results indicate that the probability of nucleation highly depends on the target temperature. Further investigation may reveal the physics behind the deposition.

5.2 Demonstration of narrow trench refill process (HARNS-damascene process)

On a silicon chip, trenches were drawn using a rapid electron beam (EB) writer (ADVANTEST F5112+VD01) with a thick EB resist (OEPR CAP-112). The chip was then etched by ICP-RIE (SPTS MUC-21 ASE-Pegasus). The narrowest trench was 22.5 μm in depth and the widths were 1 μm (at the entrance) and 450 nm (at the bottom), yielding the aspect ratio of 50. The length of the trenches was 2 mm. Prior to SCFD, the sample was cleaned with sequences 1, 4, and 5 in Table 3, as well as other demonstrations. SCFD was performed on this sample (L-1) under the following conditions: $(w_{\text{Cu}}, p_{\text{ICo2}}, p_{\text{IH2}}, p_{\text{R}}, T_{\text{T}}, t_{\text{T}}) = (12 \text{ mg}, 11 \text{ MPa}, 1 \text{ MPa}, 20 \text{ MPa}, 150 \text{ }^{\circ}\text{C}, 10 \text{ min})$.

Figure 9 shows cross-sectional SEM views of the trench conformally covered with the SCFD-Cu film. The deposited thickness was uniform from the top [Fig. 9(b)] to the bottom [Fig. 9(c)]. From the SEM image, the deposition thickness was measured to be around 100 nm. The deposited Cu film had good step coverage in the trench.

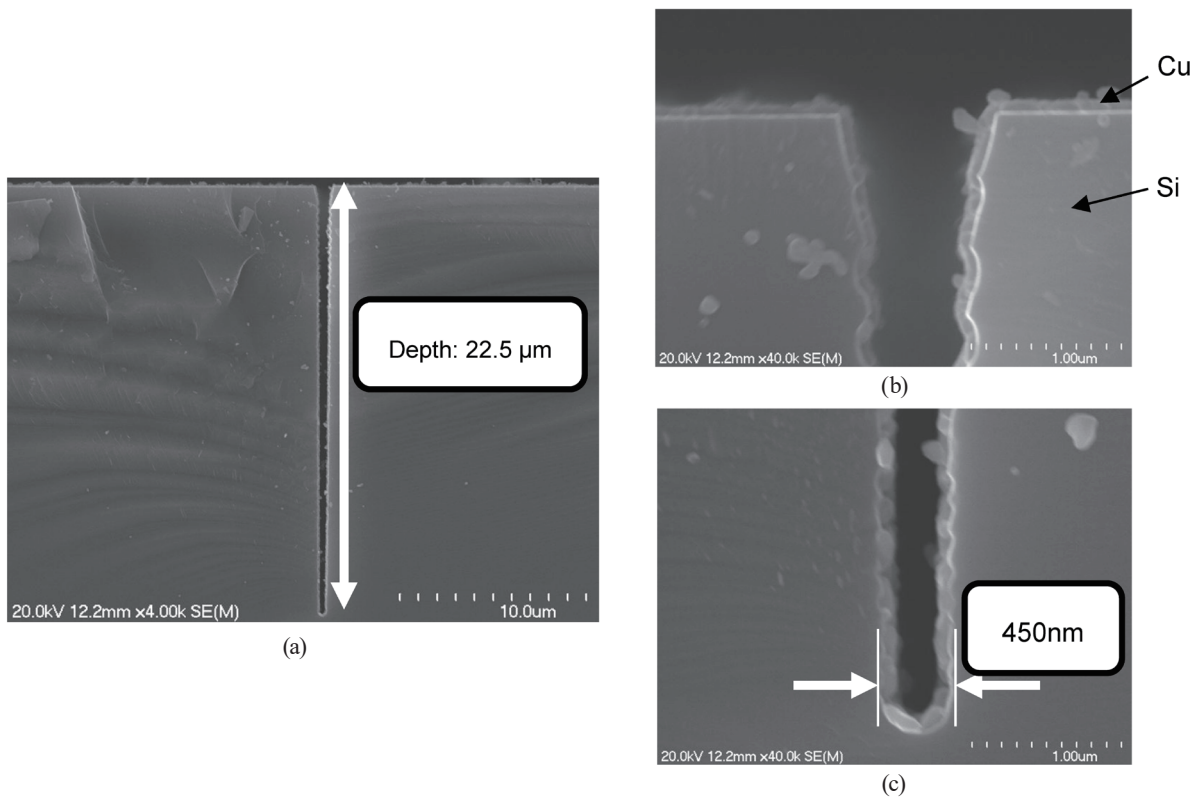


Fig. 9. SEM view of a 450-nm-wide, 22.5- μm -deep trench refilling SCFD.

6. Conclusions

A comprehensive study to increase the reliability of the Cu-SCFD process was reported. The pretreatment of the substrate was found to be particularly important. The effect of the cleaning was clarified by FE-AES and SPM analyses. It is necessary to combine organic cleaning, “piranha” cleaning, APM cleaning, and hydrofluoric acid cleaning to remove organic and metal contaminations and native oxide film from the sample surface, followed by appropriate baking to remove humidity. We have revealed a deposition condition under which a Cu film of good quality can be grown on a Si substrate. Cleaning of the chip by BHF and APM just before deposition was confirmed to be important for obtaining a high adhesion force of the deposited Cu on the surface. The nucleation density on the Si substrate was also confirmed to strongly be influenced by the target temperature T_T ; a difference of as small as 10 °C changed the nucleation morphology. Good coverage on the Si surface was obtained at the temperature T_T of 150 °C, on both a flat surface and the surface of a 450-nm-wide, 22.5- μ m-deep trench. Our achievement can contribute to the realization of HARMS/HARNS composed of Si and Cu.

Acknowledgments

This work was supported by MEXT Nanotechnology Platform. SPM was performed using the apparatus of the UTokyo Institute of Innovation, School of Engineering's Nanotechnology Platform Advanced Characterization Platform. All the other processes were done in the UTokyo VDEC Nanotechnology Platform Nanofabrication Center at Takeda Sentanchi Supercleanroom. This work was partially supported by AMED JP18hm0102060. We specially acknowledge The UTokyo VDEC and Faculty of Engineering cleanroom support teams. JSPS Kakenhi (Grant Nos. 18J10240 and 16H04345) is acknowledged.

References

- 1 F. Lärmer and A. Urban: *Microelectron. Eng.* **67** (2003) 349–355.
- 2 F. Marty, L. Rousseau, B. Saadany, B. Mercier, O. Français, Y. Mita, and T. Bourouina: *Microelectron. J.* **36** (2005) 673.
- 3 R. Beica, C. Sharbono, and T. Ritzdorf: *Proc. Electronic Components and Technology Conf.* (2008) 577–583.
- 4 Y. Mita, E. Lebrasseur, Y. Okamoto, F. Marty, R. Setoguchi, K. Yamada, I. Mori, S. Morishita, S. Inoue, Y. Imai, K. Hosaka, A. Hirakawa, M. Kubota, and M. Denoual: *Jpn. J. Appl. Phys.* **56** (2017) 06GA03.
- 5 J.-M. Blackburn, D.-P. Long, A. Cabanas, and J.-J. Watkins: *Science* **294** (2001) 141.
- 6 T. Momose, A. Kondo, T. Kamiya, H. Yamada, J. Ohara, Y. Kitamura, H. Uchida, Y. Shimogaki, and M. Sugiyama: *J. Supercritical Fluids* **105** (2015) 193.
- 7 D. Edelstein, J. Heidenreich, R. Goldblatt, W. Cote, C. Uzoh, N. Lustig, P. Roper, T. McDevitt, W. Motsifft, A. Simon, J. Dukovic, R. Wachnik, H. Rathore, R. Schulz, L. Su, S. Lucet, and J. Slattery: *Proc. Technical Digest of International Electron Devices Meeting (IEDM)* (1997) 773–776.
- 8 Z. Li, A. Rahtu, and R. G. Gordon: *J. Electrochemical Soc.* **153** (2006) C787.
- 9 E. Ota, X. Hurtaud, T. Momose, A. Higo, and Y. Mita: *Proc. 34th Sensor Symposium* (2017) 01pm4-PS130 (in Japanese).
- 10 N. Usami, A. Higo, E. Ota, and Y. Mita: *Proc. 35th Sensor Symposium* (2018) 01pm1-PS183 (in Japanese).
- 11 T. Momose, T. Uejima, H. Yamada, Y. Shimogaki, and M. Sugiyama: *Jpn. J. Appl. Phys.* **51** (2012) 056502.
- 12 A. Cabañas, X. Shan, and J. J. Watkins: *Chem. Mater.* **15** (2003) 2910.
- 13 A. H. Romang and J. J. Watkins: *Chem. Rev.* **110** (2010) 459.
- 14 E. Kondoh: *Jpn. J. Appl. Phys.* **44** (2005) 5799.

- 15 A. Cabañas, D. Long, and J. J. Watkins: Chem. Mater. **16** (2004) 2028.
- 16 T. Uejima, T. Momose, M. Sugiyama, E. Kondoh, and Y. Shimogaki: J. Electrochem. Soc. **160** (2013) 3290.
- 17 M. Watanabe, Y. Takeuchi, T. Ueno, M. Matsubara, E. Kondoh, S. Yamamoto, N. Kikukawa, and T. Suemasu: Jpn. J. Appl. Phys. **51** (2012) 05EA01.
- 18 A. Teraoka, M. W. Å, Y. Nabetani, and E. Kondoh: Jpn. J. Appl. Phys. **4** (2013) 05EA02.
- 19 M. Watanabe and E. Kondoh: Microelectron. Eng. **120** (2014) 59.
- 20 M. Rasadujjaman, M. Watanabe, H. Sudoh, H. Machida, and E. Kondoh: Microelectron. Eng. **137** (2015) 32–36.
- 21 T. Momose, M. Sugiyama, E. Kondoh, and Y. Shimogaki: Appl. Phys. Express **1** (2008) 0970021.
- 22 M. Matsubara, M. Hirose, K. Tamai, Y. Shimogaki and E. Kondoh: J. Electrochem. Soc. **156** (2009) H443.
- 23 E. Kondoh and J. Fukuda: J. Supercrit. Fluids **44** (2008) 466.
- 24 B. Giroire, M. A. Ahmad, G. Aubert, L. Teule-Gay, D. Michau, J. J. Watkins, C. Aymonier, and A. Poulon-Quintin: Thin Solid Films **643** (2017) 53.
- 25 W. Kern and D. A. Puotinen: RCA Review **31** (1970) 187.

About the Authors



Naoto Usami received his B.E., M.E., and Ph.D. degrees in electrical engineering from The University of Tokyo, in 2014, 2016, and 2019, respectively. In 2014, he served as a project manager for the realization of Deep Space Sculpture “DESPATCH”, which was part of the ARTSAT project. His current interests include antenna design, micro wireless power transfer, micro- and nanofabrication, and reconfigurable autonomous distributed microsystems. (usami@if.t.u-tokyo.ac.jp)



Etsuko Ota received her B.E. degree in electrical engineering from Ibaraki University, Japan, in 1985. From 1985 to 1993, 1996 to 1998, and 1999 to 2001, she worked on the development of a stepper system at Nikon Corporation, Japan. From 2008 to 2017, she was a research assistant at The University of Tokyo. Since 2017, she has been a senior engineer at MEXT Nanotechnology Platform UTokyo Nanofabrication Site. Her research interests are in microfabrication, surface analysis, and sensors. (ohta@if.t.u-tokyo.ac.jp)



Takeshi Momose received his B.S. degree from The University of Tokyo, Japan, in 2003 and his M.S. and Ph.D. degrees from The University of Tokyo, Japan, in 2005 and 2009, respectively. From 2011 to 2016, he was an assistant professor at The University of Tokyo, Japan. Since 2016, he has been a lecturer at The University of Tokyo. His research interests are in the development of thin film processes. (momo@dpe.mm.t.u-tokyo.ac.jp)



Akio Higo received his B.E. degree from Seikei University, Tokyo, Japan, in 2002 and his M.E. and Ph.D. degrees from the Department of Electrical Engineering, The University of Tokyo, Tokyo, Japan, in 2004 and 2007, respectively. From 2007 to 2012, he was an assistant professor at the Research Center for Advanced Science and Technology, and from 2012 to 2016, he was an assistant professor at the World Premier Initiative Advanced Institute for Materials Research, Tohoku University, Sendai, Japan. Since 2016, he has been a project lecturer in the D2T research division, VLSI Design and Education Center, The University of Tokyo. His research interests are in NEMS/MEMS, nanolithography for III-V materials and silicon, and silicon photonics. (higo@if.t.u-tokyo.ac.jp)



Yoshio Mita is an associate professor of the Department of Electrical Engineering and Information Systems, Graduate School of Engineering, The University of Tokyo (UTokyo). He obtained his BE (1995), ME (1997), and PhD (2000) degrees from the Department of Electrical and Electronic Engineering, UTokyo. He served as an assistant professor of VLSI Design and Education Center (VDEC), UTokyo, and was promoted to lecturer in the Department of Electrical Engineering in 2001 and then to associate professor in 2005. Since 2012, Dr. Mita has been a manager of a Ministry of Education (MEXT)-supported National Nanotechnology Platform UTokyo open nanofabrication site, operated jointly by VDEC and the Faculty of Engineering. His research interests include CMOS and MEMS integration technology, such as a high-voltage-generating photovoltaic for autonomous distributed microsystems. (mems@if.t.u-tokyo.ac.jp)

https://www.if.t.u-tokyo.ac.jp/index_en.html

<http://www.vdec.u-tokyo.ac.jp/English/index.html>